Repulsive to attractive interaction quenches of 1D Bose gas in a harmonic trap

Wladimir Tschischik and Masudul Haque
Max-Planck-Institut für Physik komplexer Systeme,
Nöthnitzer Strasse 38, 01187 Dresden, Germany
(Dated: October 18, 2018)

We consider quantum quenches of harmonically trapped one-dimensional bosons from repulsive to attractive interactions, and the resulting breathing dynamics of the so-called 'super-Tonks-Girardeau' (sTG) state. This state is highly excited compared to the ground state of the attractive gas, and is the lowest eigenstate where the particles are not bound or clustered. We analyze the dynamics from a spectral point of view, identifying the relevant eigenstates of the interacting trapped many-body system, and analyzing the nature of these quantum eigenstates. To obtain explicit eigenspectra, we use Hamiltonians with finite-dimensional Hilbert spaces to approximate the Lieb-Liniger system. We employ two very different approximate approaches: an expansion in a truncated single-particle harmonic-trap basis and a lattice (Bose-Hubbard) model. We show how the breathing frequency, identified with the energy difference between the sTG state and another particular eigenstate, varies with interaction.

arXiv:1411.5544v1 [cond-mat.quant-gas] 20 Nov 2014

I. INTRODUCTION

The traditional focus of many-body quantum physics has been on the ground state and low-energy parts of the eigenspectrum. This is well-justified in solid-state systems which are usually in contact with a thermal bath and typically relax fast to low-energy sectors. As a result, parts of the many-body eigenspectra away from the low-energy sector were generally considered to be irrelevant.

In recent years, the perspective has changed dramatically, largely due to new experimental possibilities with cold atom gases [1], which have promoted the study of non-equilibrium situations in *isolated* quantum systems [2]. In an isolated situation, energy conservation ensures that a system with an initially high energy will not reach the low-energy parts of the spectrum; the low-energy sector may thus be unimportant. One well-known example is that of 'repulsively bound' states of lattice particles [3, 4]. Eigenstates with particles clustered together have larger energy for repulsive interactions, but bound states may be unable to decay due to energy conservation. Eigenstates with bound nature will determine the dynamics if a system is initially prepared with bound states, even if such eigenstates are high in energy.

The so-called super-Tonks-Girardeau (sTG) state, which will be the focus of this paper, concerns the reverse situation of attractive interactions, for bosons confined to one dimension. Now, clustered states are lower in energy, and eigenstates without bound states are high up in energy. Again, in isolation, once the system is initiated in a 'gas-like' state, such high-energy eigenstates determine the dynamics and the lower-energy cluster states play no role. In Ref. [5], the lowest gas-like state of a one-dimensional trapped Bose gas was excited by starting from the ground state of the gas with repulsive interaction and rapidly switching the sign of the interaction. For large negative magnitudes, the lowest gas-like state is called the sTG state. We will extend the definition slightly and refer to the lowest gas-like state at any negative interaction as the sTG state.

In this work, we study the properties of the sTG state and the result of a repulsive-to-attractive interaction quench, in the presence of an explicit harmonic trap. We provide a *spectral* description of the trapped system and of the breathing mode dynamics excited by the quench.

The continuum Lieb-Liniger Hamiltonian has infinite Hilbert space dimension; we address it by two different approximations with finite Hilbert space dimensions: (1) we approximate it by expressing the multi-particle basis in terms of a truncated basis of single-particle harmonic oscillator eigenstates, and (2) we study a tight-binding lattice system (Bose-Hubbard model) with a harmonic trap. For these model Hamiltonians we characterize the full energy spectrum of multi-boson systems as a function of the two-body interaction. In both systems, there are eigenstates where some or all particles are (anti-)bound, so that there is a pronounced, roughly linear, dependence of such eigenenergies on the interaction strength. Eigenstates without such binding have eigenenergies that look mostly horizontal when plotted against interaction. We refer to the first type as 'cluster' or 'non-horizontal' states, and the second type as 'gas-like' or 'horizontal' states. We identify the sTG state as the lowest 'horizontal' state.

We identify the eigenstates that are excited in a repulsive-to-attractive quench. In addition to the sTG state, the important eigenstates are the ground state of the attractive system and the third horizontal state above the sTG state. This latter eigenstate is responsible for setting the breathing mode frequency at large interactions; we will call it the 'breathing' eigenstate. We present the interaction dependence of the frequency determined by this eigenstate, and explain this dependence through an examination of the natures of the first few 'horizontal' eigenstates.

The breathing mode frequency is twice the trapping frequency, $2\omega_0$, at zero and $\pm\infty$ interactions. For positive interactions, it is known to fall below this value at intermediate interactions [6, 7]. The sTG state connects to the ground state of the repulsive case at zero

and $\pm\infty$ interactions, and therefore also has breathing frequency $2\omega_0$ in these limits. However, at intermediate attractive interactions, the breathing frequency was predicted [8] using local density approximation calculations to rise above $2\omega_0$; this was observed in the experiment [5]. Our results in this paper give a spectral view of this phenomenon: we are able to identify the eigenstates in the interacting few-body spectrum whose energy difference from the sTG state serves as the breathing mode state. We find that the relevant eigenstate is different for small and large negative interactions: the third 'horizontal' eigenstate plays this role at large interactions but the ground state plays this role at smaller interactions.

The sTG state was first proposed in Ref. [8] using quantum Monte Carlo methods. Combined with a local density approximation for trapped systems, this work predicted the non-monotonic interaction-dependence of the breathing mode. Ref. [9] presented multi-configuration time-dependent Hartree calculations for the structure of eigenstates of the attractive trapped 1D Bose gas. The experiment of Ref. [5] created the sTG state, and measured its breathing mode frequency, using a quench from repulsive to attractive interactions. Subsequently, the *homogeneous* sTG gas has been studied using the Bethe ansatz [10–15] and exact diagonalization [16]. The TEBD simulations of Ref. [17] use a weak trap but do not study trap-generated features like collective modes. Analogs of the sTG state in several other systems have been studied theoretically, e.g., in spinor Bose gases [18], in dipolar Bose gases [19], and in fermionic systems [20].

While the homogeneous case has been studied in much greater detail, the experimental realization of the sTG state is in a harmonic trap and the main diagnostic is the behavior of the breathing mode excitation, which is only well-defined for a trapped system. The previous treatments of collective modes in trapped systems used a local density approximation on the results from equilibrium calculations with a homogeneous system [8, 11]. In contrast, our work provides a direct study of the breathing mode in the trapped system, both through real-time evolution after the quench and through a detailed study of the spectrum of the trapped attractive system.

In Sec. II we introduce the two approximate model Hamiltonians that we use. In Sec. III we describe the full spectrum and the position of the sTG state within the full spectrum. In Sec. IV we consider quenches from repulsive to attractive interactions that preserve the magnitude of the interaction. We show which eigenstates are excited in such quenches. In Sec. V we study the dependence of the breathing mode frequency on the interaction strength, following both the energy difference between relevant eigenstates and the frequency extracted from real-time dynamics. Sec. VI provides a summary and discussion, and some details are provided in the Appendices.

II. MODEL AND HAMILTONIAN

We are interested in bosons in one-dimensional traps, interacting through contact interactions, i.e., the trapped Lieb-Liniger (LL) [21] gas. The Hamiltonian is

$$H_{LL} = \sum_{i=1}^{N}\left[-\frac{\hbar^2}{2m}\frac{\partial^2}{\partial x_i^2} + \frac{m\omega_0^2}{2}x_i^2\right] + g\sum_{1\le i<j\le N}\delta(x_i-x_j)\,, \quad (1)$$

where N is the number of bosons in the trap, g is the interaction strength, m is the boson mass, and ω_0 is the trapping frequency. Ultracold bosonic atoms behave as a 1D system when the transverse degrees of freedom are frozen out by tight confinement [22, 23]. The system of Lieb-Liniger bosons in a harmonic trap has by now been realized in multiple cold-atom laboratories [5, 24].

The continuum LL Hamiltonian above has an infinite-dimensional Hilbert space. In this work, we address the energy spectrum of the LL Hamiltonian by two different finite-dimensional approximations.

One approach is to represent the many-particle basis in terms of occupations of single-particle harmonic oscillator eigenstates, with a truncation of the single-particle states (Appendix A). The resulting Hamiltonian, which we will refer to as the harmonic oscillator (HO) Hamiltonian, is

$$H_{HO}^{M} = \sum_{k=1}^{M}\left(\frac{1}{2}+k\right)n_k + g\sum_{\substack{k,l,\\ m,n=1}}^{M} f_{klmn}a_k^\dagger a_l^\dagger a_m a_n\,. \quad (2)$$

Here $a_k^\dagger$, a_k, $n_k = a_k^\dagger a_k$ are bosonic operators for the single-particle harmonic-oscillator mode k, and f_{klmn} is an integral over four harmonic oscillator eigenfunctions. In this representation, the kinetic and potential parts of the Hamiltonian are diagonal, and the interaction part is off-diagonal. The first M single-particle states are used. The resulting spectrum contains a finite number, $\binom{M+N-1}{N}$, of eigenstates. In the limit $M\to\infty$, the Hamiltonian (2) is identical to Lieb-Liniger Hamiltonian (1). For full numerical diagonalization, we restrict to $M\le 100$. The influence of the cutoff M on the spectrum is discussed in Appendix A. This approach to trapped interacting bosons has been used, e.g, in Refs. [25, 26].

The other approach is to address the physics of the LL gas with a 1D lattice Bose-Hubbard (BH) Hamiltonian. This tight binding Hamiltonian describes bosons with on-site interactions and captures continuum physics for small fillings. The BH Hamiltonian with a trapping potential is

$$H_{BH} = -J\sum_{i=1}^{L-1}\left(b_i^\dagger b_{i+1} + b_{i+1}^\dagger b_i\right) + \frac{U}{2}\sum_{i=1}^{L} n_i(n_i-1) + \sum_{i=1}^{L} V(i)n_i, \quad (3)$$

where b_i, $b_i^\dagger$ are the bosonic operators for site i. The Hilbert space is finite because we use a finite chain of L sites, with $N \ll L$. The parabolic trapping potential

$$V(i) \;=\; \frac{1}{2}k\left(i - \frac{L+1}{2}\right)^2 \tag{4}$$

is centered at the midpoint of the chain. For low enough densities, we can approximate the cosine dispersion of a lattice particle by a quadratic dispersion; this "effective mass approximation" $m^* = \frac{1}{2J}$ ascribes a continuum mass to lattice particles, so that we can relate our trapping strength k to the trapping frequency of a continuum trapping potential $\frac{1}{2}m\omega_0^2 x^2$:

$$\omega_0 = \sqrt{2kJ}. \tag{5}$$

We will take this to be the definition of the trapping frequency ω_0 on the lattice.

The continuum 1D Bose gas is commonly characterized by the ratio γ between interaction and kinetic energies. For a homogeneous continuum gas, $\gamma = mg/(\hbar^2 n)$, where n is the density. For the dilute BH system γ is equal to $\gamma = U/J$ [27]. Thus, if we want to compare a low-filling lattice BH gas with a continuum gas having the same γ, we would have

$$U = \frac{mJ}{\hbar^2 n} g\,. \tag{6}$$

The correspondence is density dependent. Thus, in the trapped case of interest in this work, where the density n is not constant, there is no direct correspondence between g and U. Nevertheless, we believe that the comparisons between the spectra and dynamics of the two systems, which we present in this work, are useful and informative.

In the following, for the BH system, we use $J = \hbar = 1$ and therefore measure energy [time] in units of the tunnel coupling J [inverse tunnel coupling $1/J$]. For the continuum HO Hamiltonian we measure energy in units of the trapping frequency ω_0, time in units of $T_0 = 2\pi/\omega_0$, and length in units of the harmonic oscillator length $\sqrt{\hbar/m\omega_0}$.

III. BAND STRUCTURE IN SPECTRUM AND LOCATION OF STG STATE

In this section we describe the energy spectrum for the two finite-dimensional Hamiltonians, the lattice BH Hamiltonian and the HO Hamiltonian. In particular, we focus on the location of the sTG state. Ref. [9] provides similar (but not equivalent) information.

A. Bose-Hubbard Hamiltonian H_{BH}

We begin with the BH Hamiltonian in a harmonic trap. For illustration, Fig. 1 shows the energy spectrum of a BH system of $N = 2$ lattice bosons with a harmonic trap $V(i)$. At larger $|U|$, the spectrum separates into two bands. The horizontal band has states with two particles separated (gas-like states) and the band with finite slope consists of L eigenstates in which the boson pair is spatially bound (bound or cluster states). Cluster states have larger energy for repulsive interaction. In contrast, for attractive interactions, the ground state is a cluster state.

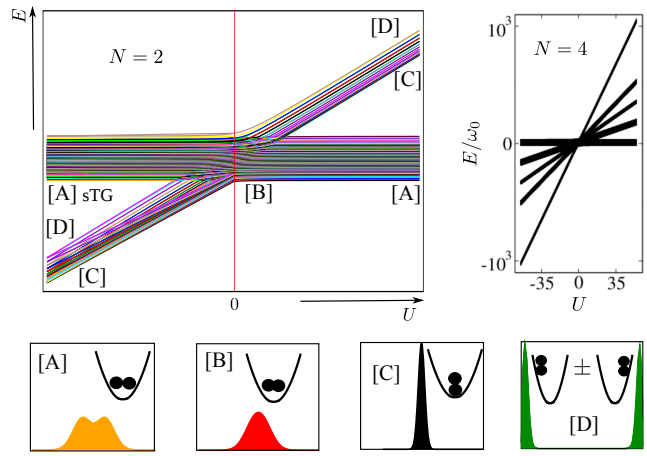

FIG. 1. Energy spectrum of lattice BH Hamiltonian. (Top left) Sketch for $N = 2$ bosons. The nature of the eigenstates in different regions of the spectra, marked [A] through [D], are shown in the lower row. Each panel in the lower row displays eigenstates in two different ways: using density profiles (filled curves) and using cartoons showing probable positions of the two particles. (Top right) Spectrum for $N = 4$ particles using $L = 20$ sites and $k = 0.05$.

Unlike a Bose-Hubbard chain without a trap, the levels near the bottom of each band are roughly equally spaced with spacing $\hbar\omega_0$, because the lower parts of each band resembles the physics of a trapped continuum system, provided the filling is small enough.

For larger number of particles the number of bands increases. Individual bands correspond to states with different-size clusters, e.g., clusters of 2, 3,... , N bound bosons and possible combinations. The right panel of Fig. 1 shows the spectrum for $N = 4$ bosons with five bands.

At small attractive interactions, bands with cluster structure cross with gas-like states, making the identification and behavior of gas-like states more complicated. At large $|U|$ the bands are completely separated. This occurs when the interaction energy sets the largest energy scale, so that the effect of negative U wins over even the largest trap energy that can be gained by the particles by sitting at the edges of the lattice (states of type [D] in Fig. 1, at the top of the cluster band).

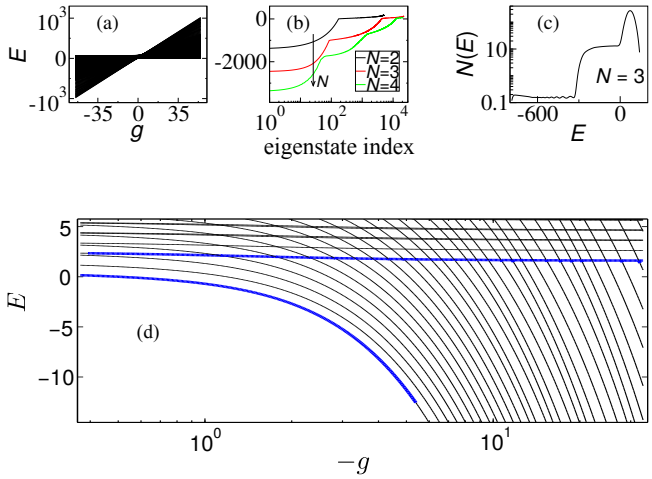

FIG. 2. (a) Energy spectrum of continuum HO Hamiltonian for $N = 4$ using $M = 20$ orbitals. In contrast to BH spectrum, the HO spectrum shows no clear separation of bands for large interaction $|g|$. (b) Eigenenergies of the HO Hamiltonian plotted in increasing order at $g = -165$, for $\{N, M\} = \{2, 100\}; \{3, 50\}; \{4, 25\}$. Note logarithmic scale for the eigenenergy index. (c) Density of states for $N = 3, M = 50, g = -54$. Eigenenergies and density of states both show plateaus, corresponding loosely to the band structure in the BH spectrum. (d) Energy spectrum of HO Hamiltonian for $N = 2, M = 20$. Thick lines indicate states having largest overlap with the ground state for $g > 0$ after $g \to -g$ quench. STG state is the lowest horizontal state.

B. Harmonic-Oscillator Hamiltonian H_{HO}

Does the band structure of the BH lattice system, described above, survive in some sense in the continuum case? This question is examined here by consideration of our second finite-dimensional Hamiltonian, the HO Hamiltonian (2).

In Fig. 2(a) we plot the spectrum for the HO Hamiltonian for $N = 4$ bosons in a trap using $M = 20$ single-particle orbitals. This could be compared to the BH energy spectrum for $N = 4$ shown in Fig. 1; the dimension of the Hilbert space is the same in the two cases. The clear band structure seen in the spectrum of the BH model is not present. However a signature of the band structure is visible in the density of eigenenergies at large $|g|$. In Fig. 2(b) we plot the eigenenergies for large negative g, in ascending order, against the index of ordering. One can see clearly a plateau structure. (Note logarithmic scale for the eigenvalue index.) Energies of cluster eigenstates strongly depend on the cutoff M; thus for small M the energies of the non-horizontal states are not reliable (Appendix A).

The spectrum of the HO Hamiltonian shows no clear band separation, nevertheless it is possible to identify the sTG state in the spectrum. In Fig. 2(d) the sTG state is visible as the lowest horizontal state, shown with a thicker line. (There is some ambiguity in the close vicinity of each level crossing.)

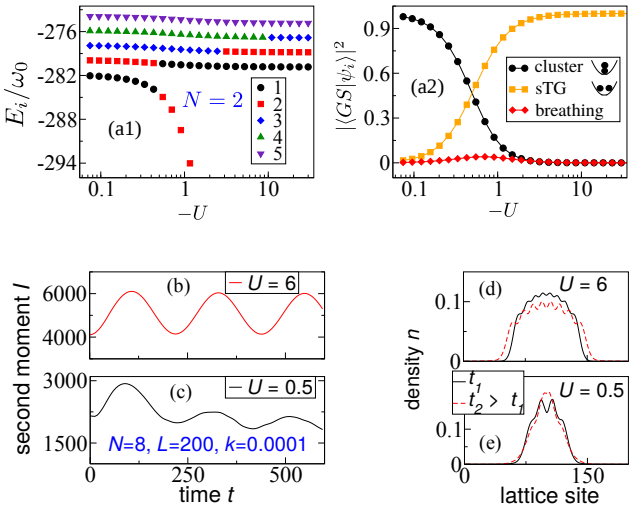

FIG. 3. $U \to -U$ quenches in the lattice BH case. (a1,a2) Data for $N = 2$, $L = 60$, $k = 0.001$. (a1) Energies of the five eigenstates of the post-quench Hamiltonian having largest overlaps with the initial groud state. (a2) Overlap magnitudes; only the largest three are shown. Outside the band-crossing region the overlap with sTG state is almost unity. (b,c) Real-time breathing dynamics after $U \to -U$ quenches, computed using TEBD; $N = 8$, $L = 200$, $k = 0.0001$. The dynamics of the cloud size, quantified using the second moment of density n, is shown. (d,e) Density distributions at some times during the post-quench dynamics.

IV. INTERACTION QUENCHES TO ATTRACTIVE REGIME

In this section we study temporal dynamics induced by repulsive to attractive interaction quenches. We start from the ground state $|GS\rangle$ of the trapped system with repulsive interaction. The sign of the interaction is then switched while keeping the same magnitude, i.e, $U \to -U$ for the BH Hamiltonian and $g \to -g$ for the HO Hamiltonian. We identify relevant eigenstates by looking at overlaps $|\langle GS|\psi_i\rangle|^2$ between the initial state $|GS\rangle$ and eigenstates $|\psi_i\rangle$ of the post-quench Hamiltonian.

We start with the lattice (BH) case. The ground state $|GS\rangle$ at positive U and its breathing mode excitation has been detailed in Ref. [7]. The density profile is Gaussian for small U; in the large-U (fermionized) regime it has the characteristic free-fermion shape with N peaks.

If Fig. 3(a), we identify the $U < 0$ eigenstates which have the largest overlaps with the initial state $|GS\rangle$. Fig. 3(a1) shows the energies of the five eigenstates with largest overlap. The three most important eigenstates are the ground state (which is a 'cluster' state at large U), the lowest 'horizontal' eigenstate (sTG state), and the third 'horizontal' eigenstate higher in energy from the sTG state. We show the overlap magnitudes with these three eigenstates in Fig. 3(a2) as a function of U.

At large negative U, the ground state is a cluster state, whose structure is very different from the initial state $|GS\rangle$. In contrast, the sTG state is close (identical) to

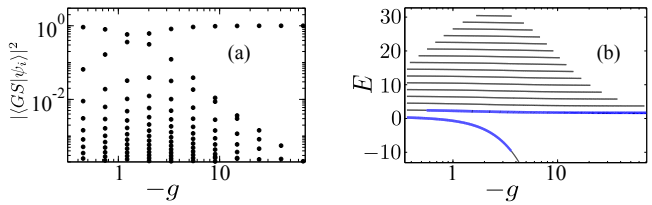

FIG. 4. $g \to -g$ quenches in the HO Hamiltonian, $N = 2$, $M = 100$. (a) Overlap of the initial ground state with eigenstates of the post-quench HO Hamiltonian. (b) Energies of the states having the overlap larger than 2×10^{-4} at different g. Thick lines indicate states with the largest overlap.

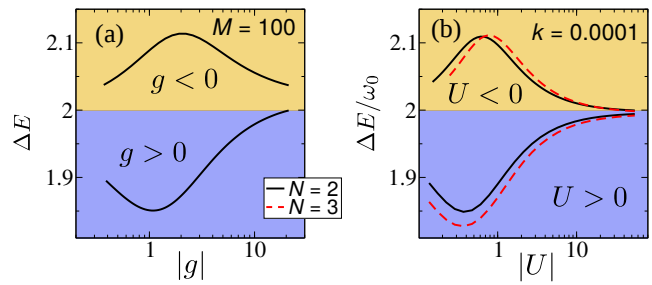

FIG. 5. Excitation energy of the breathing mode state above the sTG state (the ground state) for attractive (repulsive) interaction. The sTG state and the breathing mode state are found by looking at the largest overlaps for the interaction quenches from repulsive to attractive regimes. (a) In the HO spectrum for $N = 2$, $M = 100$. (b) In the BH spectrum for $N = 2$, $L = 250$ and $N = 3$, $L = 106$ and $k = 0.0001$.

$|GS\rangle$ for large (infinite) $|U|$. In Fig. 3(a2), this is visible through the large overlap with the sTG state and vanishing overlap with the cluster state at large $|U|$. This large overlap at large interactions has also been pointed out for the trap-free system in Refs. [11, 16]. Around $U = 0$, the state $|GS\rangle$ at positive $U > 0$ is adiabatically connected to the ground state at $U < 0$; hence the overlap with the final ground state is seen in Fig. 3(a) to be large at small $|U|$. In the region of the band crossing (small $|U|$) there are more than three states having substantial ($\geq 1\%$) overlap with initial state, although only the three with largest overlaps are shown in Fig. 3(a2).

In the BH system the band crossing part of the spectrum is qualitatively different from the part of the spectrum with separated bands. In the band-crossing region (small $|U|$), non-equilibrium dynamics following the quench will not be a simple breathing, since many states (hence many frequencies) are excited. In contrast, in the band-separated region (large $|U|$), we expect clean breathing dynamics. This is seen in the temporal dynamics pictures of Fig. 3(b,c), where we show the evolution of the second moment of the density (site occupancy) distribution $I = \sum_i n_i (i - \frac{L+1}{2})^2$, which measures the width of the bosonic cloud. The time evolution data is shown for a larger system, computed using Time-Evolving Block Decimation (TEBD) [28]. The sizes shown here are too large for us to obtain eigenstate overlap data, but the predicted feature is clearly seen: clean breathing mode for large $|U|$ and multi-frequency dynamics for smaller $|U|$ in the band crossing region.

In the HO system (Fig. 4), the "bands" are never completely separated, however the overall situation for $g \to -g$ quenches is similar, at least for $N = 2$. The overlap is largest with the ground state at smaller $|g|$, and with the sTG state at larger $|g|$. Analogous to the BH model in the band-crossing region, for moderate $|g|$ a few other "horizontal" eigenstates are excited in addition to the lowest horizontal (sTG) eigenstate.

V. BREATHING MODE OF STG STATE

A. Interaction dependence

Collective modes in a trapped system are generally associated with low-lying eigenstates. For the repulsive 1D trapped Bose gas, the eigenstate associated with the breathing mode and its excitation with respect to the ground state (which is the breathing frequency) has been detailed recently, for both lattice [7] and continuum [6] cases. The lowest excited state, at excitation energy around the trapping frequency, has odd spatial parity and corresponds to dipole oscillations (Kohn mode). There are two excited states with energy near twice the trapping frequency, one of them interaction-independent and the other deviating from $2\omega_0$ at finite interactions. This state with constant excitation energy is part of the equally spaced sequence of states related to the Kohn (dipole) mode [29]. The interaction-dependent energy level corresponds to the breathing mode. For large particle number the excitation energy of the breathing-related eigenstate at intermediate interactions approaches the mean-field prediction for the breathing frequency: $\sqrt{3}\omega_0 < 2\omega_0$ [6, 7].

For attractive interactions, the analogous picture for excitations over the sTG state is as follows. There is a dipole-mode state at energy ω_0 above the sTG state, and two states at energy near $2\omega_0$. The breathing-mode state is again the one whose excitation energy is interaction-dependent, but in this case, this excitation energy is *larger* than $2\omega_0$. The breathing mode state is thus the *third* gas-like state above the sTG state and not the *second* one above the sTG state. In addition, the situation can be complicated by the presence of many 'non-horizontal' states crossing through this energy region.

As detailed in the previous section, repulsive to attractive quenches at large $|U|$ or $|g|$ populate mainly the sTG state, but also excite breathing modes on top of the sTG state by populating the relevant breathing mode eigen-

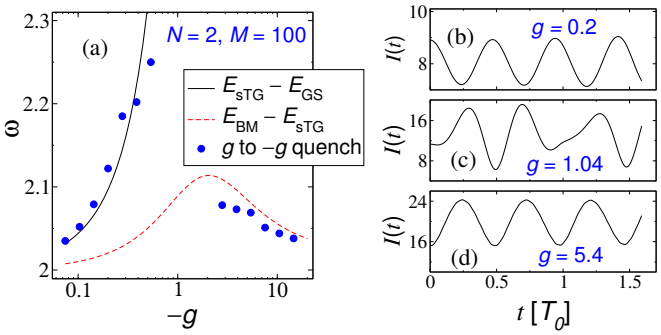

FIG. 6. HO Hamiltonian with $N = 2$ particles. (a) Frequencies extracted from time evolution of the cloud width $I(t)$ after $g \to -g$ quench (dots), compared with the energy difference between sTG and ground states (solid line), and the energy difference between sTG and breathing eigenstate (dashed, non-monotonic line). (b-d) Dynamics of the cloud radius after $g \to -g$ quench. At intermediate g, the dynamics clearly involves multiple frequencies.

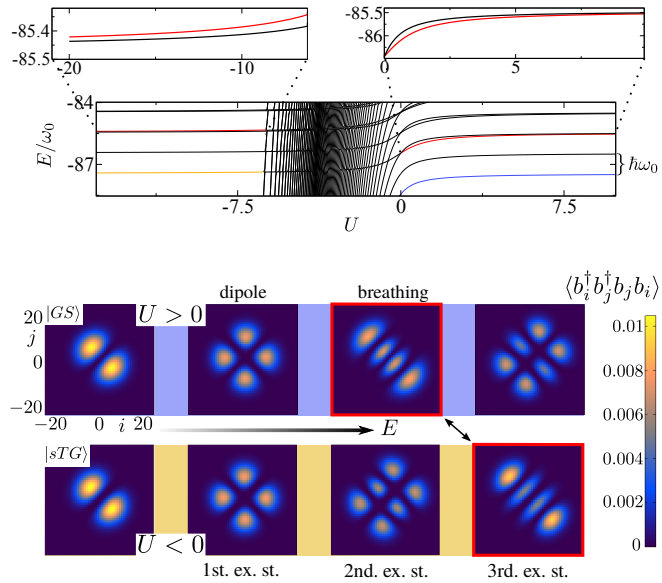

FIG. 7. (Top) Relevant part of the energy spectrum of BH Hamiltonian for $N = 2, L = 100, k = 0.001$. (Bottom) Density-density correlation $\langle b_i^\dagger b_j^\dagger b_j b_i \rangle = \langle n_i n_j \rangle - n_i \delta_{ij}$ for $N = 2$, shown as a density plot in the (i, j) plane. Here $L = 100, k = 0.001$ and $|U| = 10$. Upper panels show four lowest-energy eigenstates for $U > 0$. Lower panels show four lowest gas-like states for $U < 0$. The breathing mode eigenstate is the third state on the $U > 0$ side and the fourth gas-like state on the $U < 0$ side.

state. Thus, looking at the energy difference between the two gas-like states with highest overlaps, we can identify the excitation energy of the breathing mode eigenstate at various interaction strengths. In Fig. 5 we show the excitation energy of the breathing mode state ΔE relative to the sTG state. The excitation energy (breathing mode frequency) is larger than $2\omega_0$ and has a maximum at some finite value of the interaction. As in the repulsive case [6, 7], the breathing mode frequency is equal to $2\omega_0$ for zero and infinite interactions (with possible deviations in the BH case due to finite lattice filling [7]). For comparison, we also show the breathing mode frequency for the repulsive case, for both the lattice BH Hamiltonian and the continuum HO Hamiltonian.

The excitation energy of the 'breathing mode eigenstate' (third horizontal eigenstate above the sTG state) corresponds only at larger interactions to the breathing mode frequency obtained through time evolution. There are complications at small interactions, because the non-horizontal ground state plays an important role (has large overlap) in repulsive to attractive quenches. This is shown in Fig. 6, where the frequency of oscillations of the cloud size $I(t)$ after the quench is compared with energy differences in the spectrum. At larger interactions, the frequency matches the energy difference between the sTG state and the third horizontal state above it. At smaller interactions, however, the frequency follows much more closely the energy difference between the sTG state and the ground state. This is because for small positive to small negative interactions the dominant eigenstates are the sTG state and the ground state (previous section). There is an intermediate interaction range where the dynamics clearly involves multiple frequencies and it is difficult or impossible to assign a single frequency to the evolution of $I(t)$.

B. Structure of 'horizontal' eigenstates

The top panel of Fig. 7 shows the relevant part of the BH spectrum for $N = 2$ particles. The second and third horizontal states above the sTG both have around $2\omega_0$ higher energy than sTG state. As opposed to the repulsive case where the breathing mode is associated with the second excited state and the third excited state is the Kohn-related eigenstate [7], in the sTG case the breathing mode is associated with the *third* horizontal excited state while the *second* horizontal excited state is Kohn-related and has approximately interaction-independent energy compared to the sTG state.

The structure of eigenstates can be visualized through the *density-density correlation* (DDC) $\langle b_i^\dagger b_j^\dagger b_j b_i \rangle = \langle n_i n_j \rangle - n_i \delta_{ij}$. Fig. 7 shows plots of $\langle b_i^\dagger b_j^\dagger b_j b_i \rangle$ for two particles at large interaction, outside the band crossing region (BH Hamiltonian). The upper row of four panels show DDC for the four lowest eigenstates of repulsive ($U > 0$) bosons. The first excited state is associated with the dipole mode and the second with the breathing mode. The bottom row shows the sTG state and the three eigenstates above it; we see the same structures except that the second and third excited state structures are switched in the two cases.

The dipole mode corresponds to center-of-mass motion, i.e. oscillation of bosonic cloud around a potential

minimum. The associated eigenstate has greatest intensities at the configurations where the center of the pair is displaced, specifically, configurations with one particle is at the trap center and the other displaced. There are four such configurations in (i, j) plane, and accordingly four spots in the DDC plot. During the breathing motion center-of-mass is conserved, particles move toward and away from each other. The corresponding eigenstate is dominated by configurations where the two particles are symmetrically placed around the trap center, but at a different distance from each other than in the ground ($U > 0$) or sTG ($U < 0$) state. The DDC of the third (second) excited state for $U > 0$ ($U < 0$) is not obvious to interpret. This state is part of the "Kohn tower" — the equally spaced tower of states associated with the many-body ladder operator that describes dipole oscillations [29].

To explain heuristically why the breathing-mode eigenstate is lower (higher) than the Kohn-related mode for $U > 0$ ($U < 0$), we note from the DDC plots that the breathing-related eigenstate is marked by larger distances between the particles. For $U > 0$ ($U < 0$), this leads to lower (higher) interaction energy. This gives an intuitive explanation of why the breathing frequency for the $U > 0$ ground state is smaller than $2\omega_0$ while that of the $U < 0$ sTG state is larger than $2\omega_0$, as we have shown in Fig. 5.

VI. SUMMARY AND DISCUSSION

We have presented a study of the dynamics involved in exciting the sTG state in one-dimensional trapped bosons using quantum quenches from repulsive to attractive contact interactions. We have focused on a many-body spectral description, using exact numerical diagonalization of models with finite Hilbert space to examine the spectrum, the structure of eigenstates, and the overlaps of various eigenstates with the pre-quench state. We show that the eigenstate responsible for the breathing is the third horizontal state above the sTG state, which has a maximum above $2\omega_0$ (rather than a minimum below $2\omega_0$) at intermediate negative interactions. This perspective on the breathing mode frequency, based on the eigenspectrum, complements previous studies using local density approximations and sum rules [8, 11], and experimental measurements of the breathing mode frequency [5]. Examining the structure of the eigenstates using the density-density correlations, we arrive at an intuitive argument for the direction of the shift of the breathing frequency from $2\omega_0$. Examining explicitly the time evolution of the cloud size, we have found that at small negative interactions the breathing frequency corresponds to a different energy difference — the difference between the lowest horizontal state and the ground state of the system (Fig. 6).

A limitation of the present study is that the effects of finite M (HO Hamiltonian) or finite L (BH Hamiltonian) become severe at larger particle number. In the HO case, finite M effects affect the cluster states rather drastically (Appendix A). In the BH case, finite L limitations lead to configurations where the filling is not $\ll 1$ at the center of the trap, in which case the lattice results do not approximate continuum physics well. Most of our spectral results are obtained from full numerical diagonalization. Sparse matrix methods, which would have allowed access to larger M or L, are not well-suited to most of the calculations because the relevant energies are not at the bottom of the spectrum, and because the density of states can be large due to the presence of many 'horizontal' and 'non-horizontal' states in the same spectral region. Thus, the overlap data in Figs. 3 and 4, and the excitation energies in Figs. 5 and 6, are shown for $N = 2$ or $N = 3$ particles. For larger N, we observe similar qualitative features, but the corresponding overlaps and energies are generally not quantitatively reliable due to the finiteness effects mentioned above. While our particle numbers (2 or 3) are small, the numbers in the experiment [5] (around 20) are far too small to be justifiably approximated by mean field theories or the thermodynamic limit or local density approximations. Our small-system study of the breathing mode thus provides a valuable counterpoint to previous infinite-number studies.

The present work raises a number of open questions. First, we have found the breathing mode frequency at small and large interactions to be related to different eigenstates. This raises the question of which eigenstates are responsible for the breathing mode frequencies in the experiment [5]. Second, in both our models, we see an intermediate interaction regime where we have multi-frequency breathing oscillations; an open question is whether a similar effect might be visible in a higher-resolution experiment. Third, we have focused on breathing motion excited by interaction quenches excited by repulsive to attractive quenches. If the dynamics is excited by small interaction quenches or by small quenches of the trapping strength, one might imagine a different set of eigenstate overlaps, which may lead to differences in the size dynamics or even frequency. Finally, the collapse of the breathing mode to zero frequencies for small interactions found in the local density approximation calculations of Ref. [8] remains a mystery; it is unclear whether this should be identified with the interaction regime where we see multi-frequency dynamics, or with the interaction regime where the mixing with the ground state is responsible for the breathing dynamics of the sTG state.

ACKNOWLEDGMENTS

We thank A. Eckardt, A. M. Läuchli, A. Lazarides, R. Moessner, H.-C. Nägerl, and D. Vorberg for useful discussions. We also thank R. Moessner for collaboration on related work [7].

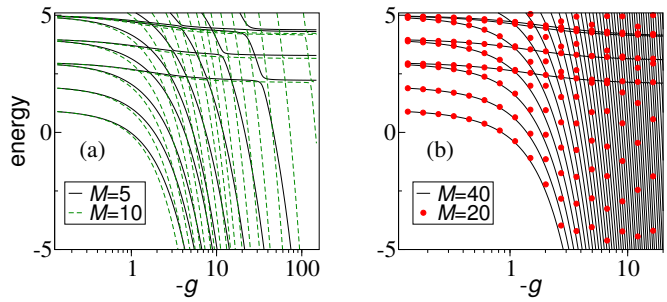

FIG. 8. Energy spectrum of the HO Hamiltonian (2) for $N = 2$: role of the cutoff M. Already with a few orbitals ($M = 5$), the spectrum contains gas-like states with very weak dependence on interaction g (note logarithmic scale). The avoided level crossings with non-horizontal states are prominent for small M. Low lying gas like states, i.e. the sTG state, converge for relatively small M. However cluster states are connected to high energy states of the non-interacting system, so that the number and energy of non-horizontal states is affected strongly by M.

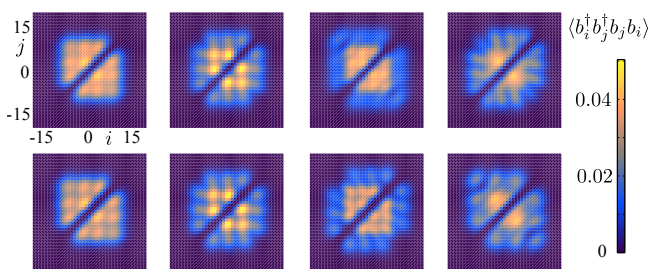

FIG. 9. Density-density correlation $\langle b_i^\dagger b_j^\dagger b_j b_i \rangle = \langle n_i n_j \rangle - n_i \delta_{ij}$ for $N = 4, L = 40, k = 0.005$. Upper panels show the four lowest-energy eigenstates for $U = 20$. Lower panels show the four lowest gas-like states for $U = -20$.

Appendix A: Expansion in free harmonic oscillator basis

The Lieb-Liniger Hamiltonian can be written in second quantization as

$$H = \int dx\, \hat{\Psi}^\dagger(x) \left(-\frac{\hbar^2 \nabla^2}{2m} + \frac{1}{2} m\omega_0^2 x^2 \right) \hat{\Psi}(x) + g \int dx\, \hat{\Psi}^\dagger(x) \hat{\Psi}^\dagger(x) \hat{\Psi}(x) \hat{\Psi}(x) \,. \quad \text{(A1)}$$

Since the single-particle harmonic-oscillator eigenstates $\varphi_k(x)$ form a complete eigenbasis, the field operators can be expanded in the corresponding mode operators a_k:

$$\hat{\Psi}(r) = \sum_k \varphi_k(r) a_k. \quad \text{(A2)}$$

The Hamiltonian then takes the form (2) with $M = \infty$ and

$$f_{klmn} = \int dx\, \varphi_k^*(x) \varphi_l^*(x) \varphi_m(x) \varphi_n(x) \quad \text{(A3)}$$

These integrals can be calculated conveniently using summation representations [26, 30].

Our approximation lies in using a finite number (M) of single-particle eigenstates. The $\binom{M+N-1}{N}$ basis states can then be chosen to be $|n_1, n_2, ..., n_M\rangle$, where $n_K \in \{0, 1\}$ is the occupation of the k-th single-particle orbital and $\sum_k n_k = N$.

Fig. 8 visualizes the influence of the cutoff M on the energy spectrum of two bosons, by comparing the spectra obtained using smaller and larger M for attractive interactions. We see that the qualitative behavior of low-lying gas-like states is captured already with small M. However for small M the sTG state has large avoided crossings with cluster states; this gets corrected with increasing M. There are strong corrections to the cluster states as a function of M; the study of low energy cluster states requires large M for $g \ll -1$.

Thus, although we have an energy cutoff in the single-particle basis, the states best approximated are not the lowest-energy many-particle states, but rather the lowest gas-like states. This method is thus particularly suitable for studying the sTG state and its dynamics.

Appendix B: Density-density correlation for larger number of particles

In the main text (Fig. 7), we have described the structure of the lowest gas-like states for $N = 2$ in terms of density-density correlation functions. The order of the two states near $2\hbar\omega_0$ excitation, the breathing mode state and the 2nd Kohn-tower state, were found to be interchanged between repulsive and attractive cases.

This situation is the same for larger number of particles, although the DDC plots are less straightforward to interpret. In Fig. 9 we plot the DDC's for $N = 4$. For each j, there are generally three peaks as a function of i (and vice versa), indicating the probable positions of the other three particles.

The breathing mode eigenstate can be identified by the presence of a peak at large $j = -i$ and its mirror. As expected, this is the third eigenstate in the sequence for $U > 0$, and the fourth for $U < 0$.

[1] M. Lewenstein, A. Sanpera, V. Ahufinger, *Ultracold Atoms in Optical Lattices: Simulating quantum many-body systems*, Oxford University Press (2012). I. Bloch, J. Dalibard, and S. Nascimbéne, Nature Physics **8,**

267 (2012). I. Bloch, J. Dalibard, W. Zwerger, Rev. Mod. Phys. **80**, 885 (2008). T. Kinoshita, T. Wenger, and D. S. Weiss, Nature **440,** 900 (2006). M. Greiner, O. Mandel, T. W. Hänsch, and I. Bloch, Nature **419**, 51 (2002).

[2] A. Polkovnikov, K. Sengupta, A. Silva, M. Vengalattore, Rev. Mod. Phys. **83**, 863 (2011). J. Dziarmaga, Adv. Phys. **59**, 1063 (2010).

[3] K. Winkler, G. Thalhammer, F. Lang, R. Grimm, J. Hecker Denschlag, A. J. Daley, A. Kantian, H. P. Büchler, and P. Zoller, Nature **441**, 853 (2006).

[4] D. Petrosyan, B. Schmidt, J. R. Anglin, and M. Fleischhauer, Phys. Rev. A **76**, 033606 (2007). M. Valiente and D. Petrosyan, J. Phys. B **41**, 161002 (2008). L. Jin, B. Chen, and Z. Song, Phys. Rev. A **79**, 032108 (2009). R. A. Pinto, M. Haque, and S. Flach, Phys. Rev. A **79**, 052118 (2009). M. Valiente, D. Petrosyan, and A. Saenz, Phys. Rev. A **81**, 011601(R) (2010). R. Khomeriki, D. O. Krimer, M. Haque, and S. Flach, Phys. Rev. A **81**, 065601 (2010). A. Deuchert, K. Sakmann, A. I. Streltsov, O. E. Alon, and L. S. Cederbaum, Phys. Rev. A **86**, 013618 (2012). L. F. Santos and M. I. Dykman, New J. Phys. **14**, 095019 (2012).

[5] E. Haller, M. Gustavsson, M. J. Mark, J. G. Danzl, R. Hart, G. Pupillo, H.-C. Nägerl, Science **325**, 1224 (2009).

[6] R. Schmitz, S. Krönke, L. Cao, and P. Schmelcher, Phys. Rev. A **88**, 043601 (2013).

[7] W. Tschischik, R. Moessner, M. Haque, Phys. Rev. A **88**, 063636 (2013).

[8] G. E. Astrakharchik, J. Boronat, J. Casulleras, and S. Giorgini, Phys. Rev. Lett. **95**, 190407 (2005).

[9] E. Tempfli, S. Zöllner, and P. Schmelcher, New J. Phys. **10**, 103021 (2008).

[10] M. T. Batchelor, M. Bortz, X. W. Guan, and N. Oelkers, J. Stat. Mech.: Theory Exp. L10001 (2005).

[11] S. Chen, L. Guan, X. Yin, Y. Hao, and X. Guan, Phys. Rev. A **81**, 031609(R) (2010).

[12] Y. Hao, H. Guo, Y. Zhang, and S. Chen, Phys. Rev. A **83**, 053632 (2011).

[13] M. D. Girardeau and G. E. Astrakharchik, Phys. Rev. A **81**, 061601(R) (2010).

[14] M. Kormos, G. Mussardo, and A. Trombettoni, Phys. Rev. A **83**, 013617 (2011).

[15] M. Panfil, J. D. Nardis, and J.-S. Caux, Phys. Rev. Lett. **110**, 125302 (2013).

[16] L. Wang, Y. Hao, and S. Chen, Phys. Rev. A **81**, 063637 (2010).

[17] D. Muth and M. Fleischhauer, Phys. Rev. Lett. **105**, 150403 (2010).

[18] M. D. Girardeau, Phys. Rev. A **83**, 011601(R) (2011).

[19] M. D. Girardeau and G. E. Astrakharchik, Phys. Rev. Lett. **109**, 235305 (2012).

[20] S. Chen, X. Guan, X. Yin, L. Guan, and M. T. Batchelor, Phys. Rev. A **81**, 031608(R) (2010). M. D. Girardeau, Phys. Rev. A **82**, 011607(R) (2010). L. Guan and S. Chen, Phys. Rev. Lett. **105**, 175301 (2010). M. D. Girardeau, Phys. Rev. A **83**, 011601(R) (2011). X. Yin, X. Guan, M. T. Batchelor, and S. Chen, Phys. Rev. A **83**, 013602 (2011).

[21] E. H. Lieb and W. Liniger, Phys. Rev. **130**, 1605 (1963).

[22] M. Olshanii, Phys. Rev. Lett. **81**, 938 (1998).

[23] D. S. Petrov, G. V. Shlyapnikov, and J. T. M. Walraven, Phys. Rev. Lett. **85**, 3745 (2000).

[24] T. Kinoshita, T. Wenger, and D. S. Weiss, Science **305**, 1125 (2004). Phys. Rev. Lett. **95**, 190406 (2005); Nature (London) **440**, 900 (2006). A. H. van Amerongen, J. J. P. van Es, P. Wicke, K. V. Kheruntsyan, and N. J. van Druten, Phys. Rev. Lett. **100**, 090402 (2008). E. Haller, R. Hart, M. J. Mark, J. G. Danzl, L. Reichsöllner, M. Gustavsson, M. Dalmonte, G. Pupillo, and H.-C. Nägerl, Nature **466**, 597 (2010). T. Jacqmin, J. Armijo, T. Berrada, K. V. Kheruntsyan, and I. Bouchoule, Phys. Rev. Lett. **106**, 230405 (2011). M. J. Davis, P. B. Blakie, A. H. van Amerongen, N. J. van Druten, and K. V. Kheruntsyan, Phys. Rev. A **85**, 031604(R) (2012). A. Vogler, R. Labouvie, F. Stubenrauch, G. Barontini, V. Guarrera, and H. Ott, Phys. Rev. A **88**, 031603(R) (2013). B. Fang, G. Carleo, A. Johnson, and I. Bouchoule, Phys. Rev. Lett. **113**, 035301 (2014).

[25] T. Haugset and H. Haugerud, Phys. Rev. A **57**, 3809 (1998). T. Papenbrock and G. F. Bertsch, Phys. Rev. A **58**, 4854 (1998). G. F. Bertsch and T. Papenbrock, Phys. Rev. Lett. **83**, 5412 (1999). F. Deuretzbacher, K. Bongs, K. Sengstock, and D. Pfannkuche, Phys. Rev. A **75**, 013614 (2007).

[26] T. Papenbrock, Phys. Rev. A **65**, 033606 (2002).

[27] B. Paredes, A. Widera, V. Murg, O. Mandel, S. Fölling, I. Cirac, G. V. Shlyapnikov, T. W. Hänsch and I. Bloch, Nature **429**, 277 (2004).

[28] G. Vidal, PRL 91, 147902 (2003). G. Vidal, PRL 93, 040502 (2004). M. L. Wall and L. D. Carr, Open Source TEBD, `http://physics.mines.edu/downloads/software/tebd` (2009).

[29] L. Brey, N. F. Johnson, and B. I. Halperin, Phys. Rev. B **40**, 10647 (1989). M. Bonitz, K. Balzer, and R. van Leeuwen, Phys. Rev. B **76**, 045341 (2007).

[30] M. Edwards, R. J. Dodd, C. W. Clark, K. Burnett, J. Res. Nat. Insit. St. Tech. **101**, 553 (1996).

[31] J. W. Abraham and M. Bonitz, Contributions to Plasma Physics, **54**, 27 (2014).